doi:10.1111/j.1558-5646.2011.01269.x

THE GENETIC ARCHITECTURE OF ADAPTATION UNDER MIGRATION–SELECTION BALANCE

Sam Yeaman[1,2,3] and Michael C. Whitlock[1]

[1]*Department of Zoology, University of British Columbia, Vancouver, British Columbia V6T 1Z4, Canada*

[2]*Université de Neuchâtel. Institute of Biology. 11 Rue Emile-Argand. Neuchâtel, 2000, Switzerland*

[3]*E-mail: yeaman@zoology.ubc.ca*

Received October 6, 2010
Accepted February 15, 2011

Many ecologically important traits have a complex genetic basis, with the potential for mutations at many different genes to shape the phenotype. Even so, studies of local adaptation in heterogeneous environments sometimes find that just a few quantitative trait loci (QTL) of large effect can explain a large percentage of observed differences between phenotypically divergent populations. As high levels of gene flow can swamp divergence at weakly selected alleles, migration–selection–drift balance may play an important role in shaping the genetic architecture of local adaptation. Here, we use analytical approximations and individual-based simulations to explore how genetic architecture evolves when two populations connected by migration experience stabilizing selection toward different optima. In contrast to the exponential distribution of allele effect sizes expected under adaptation without migration (Orr 1998), we find that adaptation with migration tends to result in concentrated genetic architectures with fewer, larger, and more tightly linked divergent alleles. Even if many small alleles contribute to adaptation at the outset, they tend to be replaced by a few large alleles under prolonged bouts of stabilizing selection with migration. All else being equal, we also find that stronger selection can maintain linked clusters of locally adapted alleles over much greater map distances than weaker selection. The common empirical finding of QTL of large effect is shown to be expected with migration in a heterogeneous landscape, and these QTL may often be composed of several tightly linked alleles of smaller effect.

KEY WORDS: Chromosomal inversions, genetic architecture, genomic islands of divergence, linkage, migration–selection balance, quantitative trait loci.

Many species inhabit coarse-grained environments where selection pressures vary across their distribution and dispersal rates are low enough to permit local adaptations to emerge (Hedrick et al. 1976; Linhart and Grant 1996). Mounting evidence from studies of the loci underlying local adaptation in quantitative traits (QTL) suggests that there is considerable heterogeneity in architecture among species and among traits (Orr 2001; Slate 2005), with some traits defined by only a few QTL of large effect (e.g., pelvic girdle [Shapiro et al. 2004] and armor plating [Colosimo et al. 2004] in sticklebacks; flower architecture in *Mimulus spp*. [Bradshaw et al. 1995, 1998]; coloration in beach mice [Steiner et al. 2007]), others defined by many QTL of small effect (e.g., cold hardiness in conifers [Howe et al. 2003]; flowering time in maize [Buckler et al. 2009]), and others defined by QTL with a range of effect sizes (e.g., body shape in sticklebacks [Albert et al. 2006]). Furthermore, fine-scale dissection of large effect QTL has sometimes revealed that they contain several tightly linked genes each contributing small individual effects (e.g., skeletal traits in mice [Christians and Senger 2007]).

What factors shape this variation in genetic architecture? If there are only a limited number of genes that control the expression of a phenotypic trait under selection, then the genetic architecture of local adaptation will necessarily be constrained by the rate and size of beneficial mutations at these genes. The observation of tight linkage of small effect alleles in a single large effect QTL might also be expected if tandem gene

duplications have played an important role in the elaboration of a given phenotype. On the other hand, genetic architecture can also be shaped by evolutionary processes of natural selection and migration. Orr (1998) has shown that the distribution of allele effect sizes fixed during an adaptive walk (without migration) will be approximately exponential, even if the underlying distribution of mutation sizes is much different, whereas Griswold (2006) has shown that migration constraining the process of adaptation will cause this distribution to be skewed toward larger allele effect sizes.

As mutations with larger selection coefficients have a higher probability of contributing to adaptation and a longer persistence time under migration–selection balance in finite populations (Yeaman and Otto 2011), prolonged bouts of adaptation under gene flow could result in the gradual replacement of many small effect alleles by fewer large effect alleles, provided their effects on the phenotype are approximately interchangeable. (The expectation of an upwards bias in allele effect size in heterogeneous environments has also been suggested by Lenormand (2002) in his review of the homogenizing effect of migration.) Furthermore, if translocations, inversions, or transposable elements rearrange the physical distribution of locally adaptive alleles within and among chromosomes or if a modifier alters the rate of recombination between them, the creation of tight linkage groups can allow several small effect alleles to function effectively as a single large linkage group. Understanding how the interplay between migration, selection, recombination, and drift affects the evolution of genetic architecture and favors or disfavors these types of patterns is thus critical to interpreting the variation in QTL effect size, number, and composition seen in the natural world.

In the absence of epistasis, the interplay between divergent natural selection and migration is expected to favor architectures that minimize recombination between locally adapted alleles, as recombination breaks up the positive disequilbrium generated by selection, yielding maladaptive intermediate genotypes (Maynard Smith 1977; Pylkov et al. 1998; Lenormand and Otto 2000). Considering two populations evolving under divergent selection with migration, Kirkpatrick and Barton (2006) showed that a chromosomal inversion eliminating recombination between previously unlinked loci will experience positive selection in proportion to the number of loci involved in local adaptation and the migration rate. Interestingly, they found that the net strength of selection favoring the inversion was largely independent of the selection coefficients on the alleles involved. Although not explicitly focusing on the evolution of genetic architecture underlying quantitative traits, these studies indicate that prolonged bouts of stabilizing selection with migration should tend to favor architectures characterized by fewer, larger, more tightly linked alleles.

Most theory that explicitly explores adaptation under migration–selection balance has focused on deriving the conditions that maintain genetic polymorphism at a single locus (e.g., Haldane 1930; Wright 1931; Bulmer 1972), multiple loci (Lythgoe 1997; Spichtig and Kawecki 2004), or divergence at a quantitative trait (Hendry et al. 2001; Lopez et al. 2008), rather than examining the evolution of genetic architecture per se. To arrive at analytically tractable solutions to the migration threshold problem, the multilocus studies have typically made restrictive assumptions about the genetic architecture underlying the phenotype (e.g., diallelic loci of equal effect size), limiting the scope of inferences about how migration–selection balance shapes the distributions of effect size and number of loci. Although Spichtig and Kawecki (2004) assumed diallelic loci of equal effect size for much of their analysis of the conditions maintaining multilocus polymorphism, they also showed that when they relaxed this assumption and allowed unequal effect sizes among loci there was less polymorphism maintained, which is consistent with the expectation of fewer loci contributing to divergence under migration-stabilizing selection balance. Although this work is suggestive, they did not explicitly compare the relative fitness of genotypes with different architectures or examine the effect of linkage between loci.

The aim of this article is to examine how prolonged bouts of divergent stabilizing selection with migration, recurrent mutation, drift, and recombination affect the evolution of the genetic architecture underlying a locally adapted trait. We use a combination of individual-based simulations and analytical approximations based on work by Bengtsson (1985), Barton and Bengtsson (1986), and Yeaman and Otto (2011) to explore how the interplay of these processes affects the evolution of genetic architecture in populations adapting to different environments. Specifically, we seek to understand how the interplay between migration, selection, recombination, and drift affects the number of loci contributing to divergence, the size of alleles that diverge between populations, and their propensity to cluster together in tight linkage on a chromosome.

Analytical Approximations

SINGLE LOCUS CONTEXT

Yeaman and Otto (2011) examined a two-patch, two-allele model with migration and divergent selection, deriving several approximations to identify the conditions favoring the maintenance of polymorphism at a single locus in finite populations. Their principal finding was that the rate of change in allele frequency of a novel invading allele effectively represents the net deterministic effect of the tension between migration and selection, which they termed the "diversification coefficient," δ (increasingly diversifying as $\delta >> 0$; increasingly homogenizing as $\delta << 0$). This δ is the deviation from one of the leading eigenvalue of the transition matrix of the allele frequencies in both habitats. As such,

they showed that δ could be used to predict: (1) the probability that a new locally beneficial allele would rise to high frequency and contribute to local adaptation (hereafter, invasion probability), and (2) the threshold migration rate below which locally favored alleles tend to diverge between populations and persist for long enough to contribute to local adaptation (hereafter, critical migration threshold, m_{crit}). All else being equal, alleles with larger selection coefficients have higher values of δ, and therefore also have higher invasion probabilities, longer persistence times, and higher critical migration thresholds, all of which suggest they should be more likely to contribute to local adaptation under migration–selection–drift balance. Here, we extend the single-locus migration–selection–drift approach developed by Yeaman and Otto to make some qualitative predictions about the evolution of genetic architecture in multilocus traits, using δ as a proxy for the net diversifying effect of selection on individual alleles, and applying the critical migration threshold approach to multilocus traits. We also combine this approach with a model by Bengtsson (1985) and Barton and Bengtsson (1986) to explore the effect of linkage between locally adaptive alleles on their likelihood of contributing to local adaptation.

CRITICAL MIGRATION THRESHOLDS FOR PHENOTYPES AND ALLELES

Multilocus phenotypes diverge between populations by the gradual accumulation of locally adaptive mutations in each patch. Although selection on a phenotype may be of sufficient strength to overcome the homogenizing effects of migration, if an individual allele contributing to the phenotype has a small effect size it may be unable to make a lasting contribution to local adaptation without being homogenized by migration. To extend the critical migration threshold approach to phenotypic traits and their component alleles, we assume that the fitness of a phenotype (Z) is defined by:

$$W = 1 - \phi(\theta - Z/(2\theta))^{\gamma} \qquad (1)$$

(modified from Spichtig and Kawecki 2004), where ϕ is the strength of stabilizing selection, θ is the locally optimal phenotype (positive in one patch and negative in the other), and γ specifies the curvature of the function. By Eq. (1), an individual that is perfectly adapted in one patch experiences a disadvantage of exactly ϕ in the other patch, regardless of the value of γ, which defines the curvature of the fitness function ($\gamma>$, $=$, or <1 implies that the fitness function has a convex, linear, or concave shape around the optimum, respectively). We assume individual mutations of effect size (α) contribute additively to the phenotype, but dominance and epistasis for fitness occurs for $\gamma \neq 1$.

This fitness function can be applied to the phenotypic effect of a locally adaptive mutation of any given size to calculate its fitness relative to the resident allele. In conjunction with the approach of Yeaman and Otto (2011), we can then calculate the critical migration rate below which this new mutation would tend to be maintained, contributing to local adaptation despite the homogenizing effects of migration. This critical migration threshold (m^{α}_{crit}) is defined as the migration rate that satisfies $\delta = 1/(4N)$, the point at which the random changes in the allele's frequency caused by drift are on the same order as the systematic increases its frequency due to the net effect of the interplay between migration and selection. Following Yeaman and Otto (2011):

$$\delta = \frac{\psi}{2} + \frac{1}{2}\sqrt{\psi^2 - 4(1-2m)\frac{W_{1,Aa}}{W_{1,AA}}\frac{W_{2,Aa}}{W_{2,AA}}} - 1, \qquad (2)$$

where $\psi = (1-m)\left(\frac{W_{1,Aa}}{W_{1,AA}} + \frac{W_{2,Aa}}{W_{2,AA}}\right)$, and W_{ij} is the fitness of the j_{th} genotype in the i_{th} patch, where a is the invading allele, favored in patch 1, and A is the resident, favored in patch 2 ($W_{1,aa} = 1$; $W_{2,AA} = 1$). From this, the critical migration threshold is:

$$m^{\alpha}_{crit} = \frac{1}{\dfrac{W_{1,Aa}}{W_{1,Aa} - W_{1,AA}\left(1 + \dfrac{1}{4N}\right)} - \dfrac{W_{2,Aa}}{W_{2,AA}\left(1 + \dfrac{1}{4N}\right) - W_{2,Aa}}}. \qquad (3)$$

We also define another critical migration rate to describe the strongest possible selection on an allele associated with a single trait. The phenotypic critical migration threshold (m^{Z}_{crit}) indicates the migration rate above which even a single perfectly adapted mutation would be unable to overcome the homogenizing effects of migration.

Figure 1 shows that in cases where selection is of sufficient strength to favor divergence at the phenotypic level ($m < m^{Z}_{crit}$; horizontal dashed lines), selection may still be insufficiently strong for a mutation of size α to contribute to divergence if $m > m^{\alpha}_{crit}$ (i.e., when m falls in the area between horizontal lines and their corresponding curves). Because the allelic critical migration threshold decreases with effect size (Fig. 1), we predict that multilocus traits evolving with migration should have fewer small effect alleles than expected for traits evolving without migration (e.g., Orr 1998), as found qualitatively by Griswold (2006). Importantly, the difference between m^{Z}_{crit} and m^{α}_{crit} is much greater in smaller populations (Fig. 1); as $N \to \infty$, the difference between these thresholds decreases with the decreasing importance of drift (relative to δ). Because the decrease in m^{α}_{crit} with allele effect size is also more pronounced under weaker strengths of selection and smaller population sizes (Fig. 1), we predict this effect due the interplay of migration, selection, and drift will be much more pronounced when ϕ and/or N are small. On a quantitative level, we expect few alleles with $m^{\alpha}_{crit} < m$ to contribute to long-term adaptive divergence between populations, except when linked to other locally adaptive alleles.

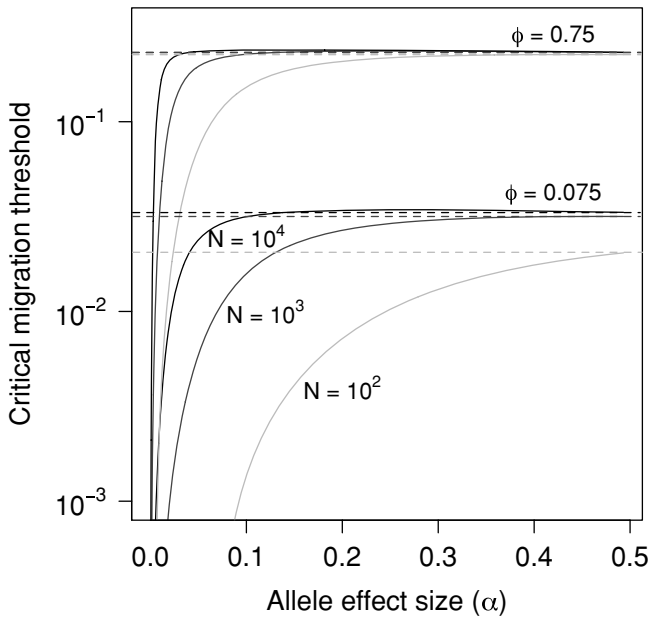

Figure 1. The allelic critical migration threshold, m^{α}_{crit} (solid curving lines) increases with allele effect size, indicating that smaller alleles cannot contribute to adaptive divergence under higher levels of migration. The phenotypic critical migration threshold (m^{Z}_{crit}; horizontal dashed lines) indicates the migration rate above which even a single perfectly adapted mutation would be unable to overcome the homogenizing effects of migration and drift (the local optima are set to $\theta = \pm 1$, so m^{Z}_{crit} occurs when $\alpha = 0.5$). Note that the difference between m^{Z}_{crit} and m^{α}_{crit} decreases with increasing population size, illustrating the importance of the interaction between migration, selection, and drift. In all cases, $\gamma = 2$, and the initial population is fixed for an allele with an effect size of $\alpha = 0$.

LINKAGE BETWEEN LOCI

If the strength of selection is too weak for a small locally adaptive mutation to overcome the homogenizing effect of migration, it may still invade and contribute to adaptation if it is linked to a larger allele at a second locus that has already diverged. Also, over time, persistent stabilizing selection with migration might favor the replacement of weakly linked pairs of alleles by more tightly linked pairs. To explore the interplay between recombination, selection, and migration, we combine the approximations for the net diversifying effect of selection developed above with a model by Bengtsson (1985) and Barton and Bengtsson (1986) for the decrease in effective migration rate at a neutral focal locus linked to a background locus under selection. They showed that a fixed difference at a background locus that is maintained by selection of strength s against immigrant types ($w_{Aa} = 1 - s$) would decrease the effective migration rate at an adjacent focal locus linked at recombination rate r by a factor of:

$$m_e = m\frac{rw_{Aa}}{1-(1-r)w_{Aa}} \tag{4}$$

This effective migration rate can be used to incorporate the effect of this linkage into the calculation of the diversification coefficient (δ) for an invading mutation at the focal locus by substituting m_e for m in the equation for δ, which we term δ_B (to represent the effect of the background; this approach could also be extended to an effect of multiple linked divergent loci, as described in Barton and Bengtsson 1986). Although this yields only an approximate solution for δ_B, due to the assumption that the background alleles are fixed in their local patches, it illustrates how the interaction between the strength of divergent selection, migration, and recombination rate influences the net strength of selection on the invasion of a second allele at a linked locus (Fig. 2).

The strength of diversifying selection on an invading allele (δ_B) increases with decreasing rates of recombination between the invading allele and the already established background allele (Fig. 2). All else being equal, higher migration rates yield the largest increases in the magnitude of δ_B as $r \to 0$ (Fig. 2), implying that the relative advantage of tight linkage between locally adaptive alleles will increase as $m \to m^{Z}_{crit}$ (with local adaptation collapsing above m^{Z}_{crit}), as found by Kirkpatrick and Barton (2006). Interestingly, higher migration rates require tighter linkage to realize these increases in δ_B, as shown by the midpoints of each curve (Fig. 2, vertical lines). Similarly, increases in δ_B occur across much higher rates of recombination under strong selection ($\phi = 0.75$) than under weaker selection ($\phi = 0.075$; Fig. 2). This occurs because stronger selection generates more linkage disequilibrium, reducing the effective migration rate over a greater distance along the chromosome (Bengtsson 1985; Barton and Bengtsson 1986). For example, when $m = 0.01$, the increase in δ_B with decreasing recombination occurs around $r \sim 0.043$ for $\phi = 0.75$ (Fig. 2A; vertical dashed lines), but around a much lower recombination rate $r \sim 0.00084$ for when selection is weaker, $\phi = 0.075$ (Fig. 2B; vertical dashed lines). As such, although we expect strong selection to maintain loosely clustered architectures, beyond a certain point there will be little fitness benefit of further increasing linkage.

Summary of analytical predictions

Based on these results, we predict that strong phenotypic selection will cause clusters of locally adapted mutations to be maintained over much wider map distances than under weaker selection. We also predict that clustering between locally adaptive alleles will be most pronounced as $m \to m^{Z}_{crit}$ (and that this pattern will break down when $m > m^{Z}_{crit}$, where no local adaptation is expected). We stress that due to the coarseness of these approximations—particularly because of the assumption of fixed differences at the linked background locus—this approach is intended more as a useful heuristic than a means of formulating quantitative estimates about the effective strength of selection on a secondary invading allele. Taken together, the analytical theory discussed above

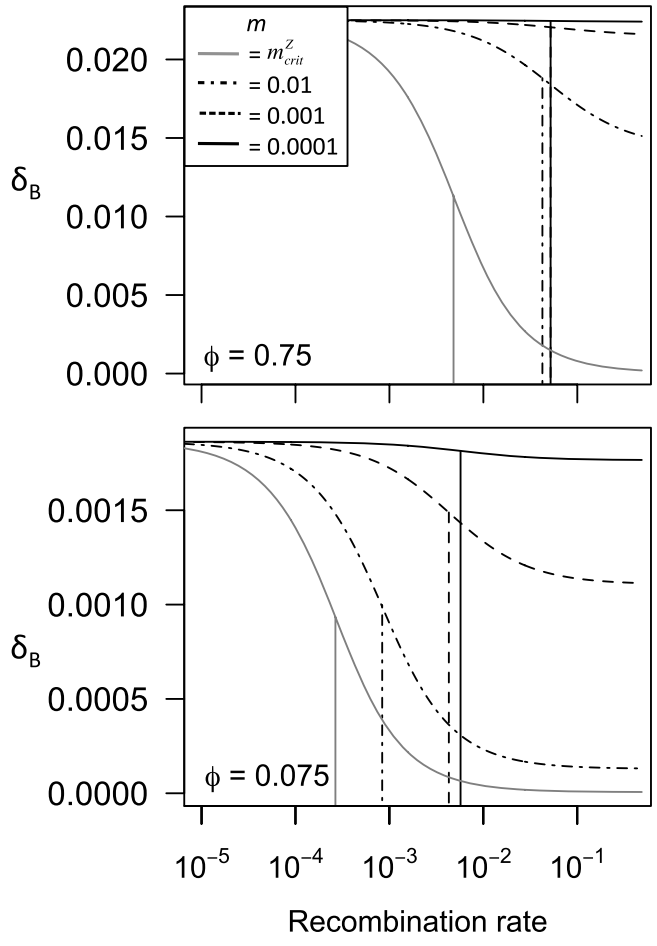

Figure 2. The net diversifying effect of selection acting on an invading allele linked to an established divergent allele (δ_B) increases with decreasing rates of recombination between them (from Eq. (4)). The transition from low to high values of δ_B occurs across higher rates of recombination with lower migration and stronger selection (vertical lines show the midpoint of each transition). An allele with higher δ_B has a higher probability of invading and a longer persistence time and is therefore more likely to make long-term contributions to adaptation. In all cases, the background allele is of size $\alpha = 0.25$ whereas the invading focal allele is of size $\alpha = 0.05$, the resident allele has $\alpha = 0$, $\theta = \pm 1$, and $\gamma = 2$; for $\phi = 0.75$, $m^Z_{crit} = 0.231$; for $\phi = 0.075$, $m^Z_{crit} = 0.0317$.

suggests there are two reasons to expect architectures with fewer, larger, and more tightly linked loci to evolve under migration–selection balance in finite populations: (1) a deterministic advantage of being tightly linked (Fig. 2 and Kirkpatrick and Barton 2006), and (2) the relatively longer persistence times and invasion probabilities of larger alleles or linkage groups in finite populations (Fig. 1 and Yeaman and Otto 2011). Although the strength of the effect due to (1) does not depend on population size, it may be more readily realized in larger populations, where drift is less important. By contrast, (2) is expected to be of greater importance in smaller populations.

Individual-Based Simulations

We used a modification of the Nemo platform (Guillaume and Rougemont 2006) to implement individual-based simulations to see how closely the observed patterns of genetic architecture under migration–selection–drift balance conform to the predictions described above (see Supporting information for source code). Individuals inhabit an environment consisting of two patches with different selection regimes connected by migration at rate m, with their absolute fitness in each patch defined by equation (1). The phenotype is defined by n additive loci arranged on a single chromosome, with recombination occurring between adjacent loci at rate r. At the beginning of each generation, diploid offspring are created by drawing parental gametes from either patch ($Pr[\text{local}] = 1 - m$; $Pr[\text{nonlocal}] = m$), which go on to survive with a probability equal to their absolute fitness (W). Offspring are created until filling the local patch to carrying capacity (N), such that the entire system effectively experiences soft selection followed by gamete migration. For simplicity, all cases discussed below use an optimum phenotype (θ) of ± 1 in each patch and a local patch population size of $N = 1000$. As mutation effect size and rate are expected to strongly influence the dynamics, we employ a flexible approach to modeling mutations, drawing their values from a Gaussian distribution with standard deviation of σ and a mean of zero. Mutations occur at a per locus rate of μ with the value of the new mutation added onto the previous allelic value at the locus. In most cases, simulations were run for 500,000 generations with summary statistics calculated every 500 generations; for simulations with low mutation rates ($\mu = 10^{-5}$) or subcritical migration rates, we ran simulations until there was no consistent change in mean phenotype (usually >1,000,000 generations). Except where otherwise noted, statistics reported in Figures 5–7 were averaged over at least 100 census points during the final portion of the simulations, with 20–40 replicates per parameter set. All simulations were initialized with mutations at 5% of the loci to provide some initial variability.

Individual "loci" in this continuum-of-alleles mutation model can be thought of either as groups of completely linked genes or a single gene subject to recurrent mutation (e.g., the *Drosophila shavenbaby* gene [McGregor et al. 2007]). The term "allele" and "locus" will be used throughout this article to simplify discussion, however it should be kept in mind that a "locus" in these simulations could represent several tightly linked genes. Under the continuum-of-alleles model, genetic architecture can evolve to mimic the genotype created by a single large allele through recurrent mutations at the same locus (hereafter "stacking") or through mutations at several tightly linked loci (hereafter "clustering"). Genetic architectures that tend to have fewer loci of larger effects and/or tighter linkage between loci contributing to divergence will be referred to as "concentrated," whereas those with more loci of smaller effects and looser linkage will be referred to as "diffuse."

An ideal simulation would include tens of thousands of loci with heterogeneous recombination rates across the genome and explore whether locally adapted mutations tended to cluster around areas of reduced recombination. As this would be computationally prohibitive, we focus instead on a single chromosome with 50 loci and examine the effect of differences in the rate of recombination between adjacent loci to represent what would occur if locally adaptive genes were restricted to areas of high versus low recombination (or equally, spaced along an entire chromosome vs. confined to a small region of the chromosome).

As multiple alleles may segregate at a single locus within each population under the continuum-of-alleles model, the most common allele at the *i*th locus in the *j*th patch is referred to as the "leading allele": α'_{ij}. The difference between leading alleles in the two patches is represented by $d = \alpha'_{i,1} - \alpha'_{i,2}$, with d_{max} referring to the size of the largest value of d at a given census point, averaged across all replicates. Individual-based simulations involve considerable stochasticity in values of d; although a large number of loci may be differentiated at any given census point, only a few of these typically make a long-term contribution to divergence. We use the term "transient" to differentiate these short-lived polymorphisms from loci with longer-lasting "stable" allelic divergence, which are given the symbol d' (defined as those loci with $d \neq 0$ for at least 32 out of 40 census points during the 20,000 generations preceding the focal census point). To represent the extent of clustering in the genetic architecture, we calculated the "clustering distance" as the average physical distance between the locus with $d'_{\max}$ and all other stable differentiated loci (i.e., absolute difference in position on the chromosome), setting this to zero if only a single locus was stably differentiated. To estimate the average size of alleles contributing to long-term divergence, we calculated the average size of d at all stable diverged loci (d'_{mean}), averaged over all replicates.

Results

EVOLUTION OF GENETIC ARCHITECTURE—THREE DOMAINS

As the migration rate increases, the system passes through two thresholds where the genetic architecture of adaptive divergence changes dramatically. When the migration rate is very low, the two populations evolve largely independently of each other, rapidly approaching their local optima and then gradually cycling through different combinations of alleles with opposing effects that sum to yield a locally optimal phenotype, which likely replace each other due to drift, as different allelic configurations yielding similar phenotypes would be nearly neutral with respect to each other (Fig. 3A). Although both populations contain genotypes that are well adapted to their local optima within the first few thousand generations of the simulations (as indicated by the black line in Fig. 3D), as time progresses, the genetic architectures of the two populations diverge further and further with increasingly large effect size alleles at the locus with the largest value of d (d_{max}; Fig. 3D; red). Eventually, the size of d_{max} surpasses the value conferring optimal adaptation in each patch, but is compensated by alleles with opposing effects at other loci, whose values of d continue to increase in absolute size through repeated mutations (Fig. 3D; blue). Although the recombinant F2 offspring of a mating between individuals from the different patches would have somewhat reduced fitness, such matings are infrequent enough at low migration that selection is too weak to prevent the architectures from drifting apart, ultimately leading to speciation. Similar behavior is seen in completely allopatric populations, when $m = 0$ (results not shown).

When m is above the drift threshold but below the selection threshold ($m < m^Z_{crit}$), migration is frequent enough to entrain the architectures of the two populations, such that at the end of the simulations, they differ at only a few loci necessary to build a locally adaptive phenotype (Figs. 3B,E). In the example shown in Figure 3B, the small mutation effect size and high mutation rate result in the gradual stacking of mutations (indicated by the gradual increase in d_{max} and lack of increase in d at all other loci), yielding an architecture with a single locus conferring most of the adaptive divergence between the populations and transient divergence contributed by small effect alleles at other loci. At the outset of the simulations in this domain, distributions of the sizes of alleles contributing to divergence were quite similar to the exponential distribution expected by Orr (1998) in the absence of migration (Fig. 4). But as time progressed, the distribution of fixed differences between populations gradually shifted toward a strongly bimodal distribution with transient small alleles and long-lived large alleles contributing to divergence (Fig. 4).

Above m^Z_{crit}, migration is too strong to permit local adaptation and transient differences in the genetic architectures of the two populations are quickly homogenized (Fig. 3C,F). The interaction between selection and drift determines the threshold migration rates at which the system transitions through these three phases, from effective allopatry (very low m), to migration–selection balance where architectures are entrained but locally adapted ($0 << m < m^Z_{crit}$), to homogenization of differences between populations ($m^Z_{crit} < m$).

The remainder of this article will focus on evolution in the middle of these three domains (i.e., Fig. 3B,E), examining the impacts of mutation rate and effect size, selection, and recombination on the architecture of local adaptation. Perhaps the most pronounced and unexpected result from the multilocus simulations is the robustness of very concentrated architectures, often characterized by a pair of large alleles at a single locus that contribute most of the adaptive trait divergence between

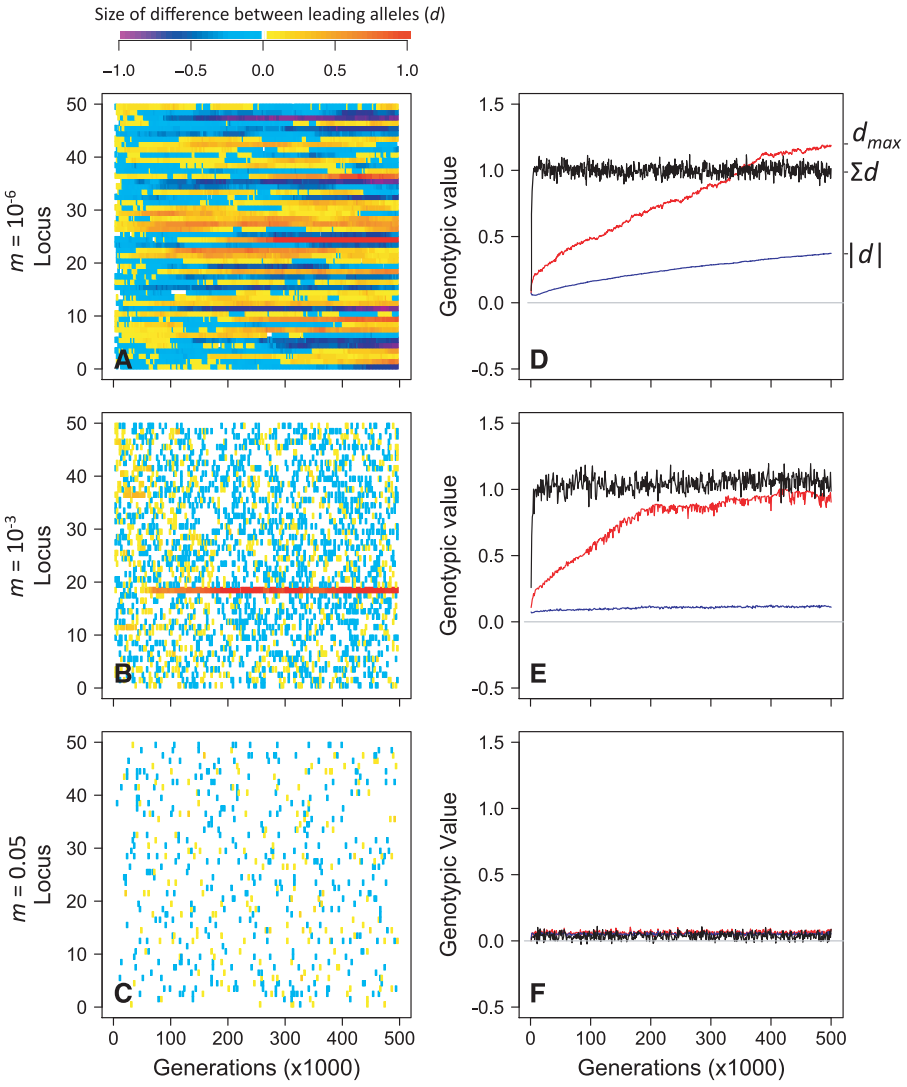

Figure 3. Evolution of genetic architecture over time at low ($m = 10^{-6}$; A and D), intermediate ($m = 10^{-3}$; B and E), and high ($m = 0.05$; C and F) levels of migration. Panels (A–C) show the difference in the size of the leading alleles (d) at each of the 50 loci for a single simulation replicate. White space signifies no differentiation between patches at that locus, whereas colors indicate the magnitude of d as shown in the legend. (Values of $|d| > 1$ are truncated to ± 1 for clarity). For these simulations, the local optima are set to $\theta = \pm 1$, such that a single locus with $d = 1$ can cause both diploid populations to be perfectly adapted to their local conditions. Panels (D–F) show summary statistics describing the genetic architecture, averaged over 20 simulation replicates: the average size of largest allelic difference at any locus, d_{max} (red); the average taken over the absolute values of d at all loci (blue); and sum of values of d across all loci (black). In all cases, $\mu = 10^{-4}$, $\sigma = 0.05$; $r = 0.02$, $n = 50$, $\phi = 0.075$, $N = 1000$.

populations. Highly concentrated architectures much like those shown Figures 3B and 4 are commonly found across a wide range of parameter sets; the following sections show how variations in mutation, migration, selection, and recombination can lead to variations on this general theme.

STRENGTH OF SELECTION AND RECOMBINATION RATE

The analytical theory developed above predicts that genetic architectures should be increasingly concentrated as $m \to m^{Z}_{crit}$, and that when clusters of locally adapted alleles occur, they should be restricted to a smaller map distance when selection is weaker (Fig. 2). The patterns observed in the individual-based simulations are consistent with these qualitative predictions. The number of differentiated loci and the average clustering distance both decrease with increasing migration rates, with the most concentrated architectures occurring when m is just below m^{Z}_{crit} (Fig. 5). When selection is stronger ($\phi = 0.75$), there is less advantage of completely clustered or stacked architectures (as per Fig. 2), and clusters of locally adapted alleles occur over larger distances of the simulated chromosome (Fig. 5C). When the rate of

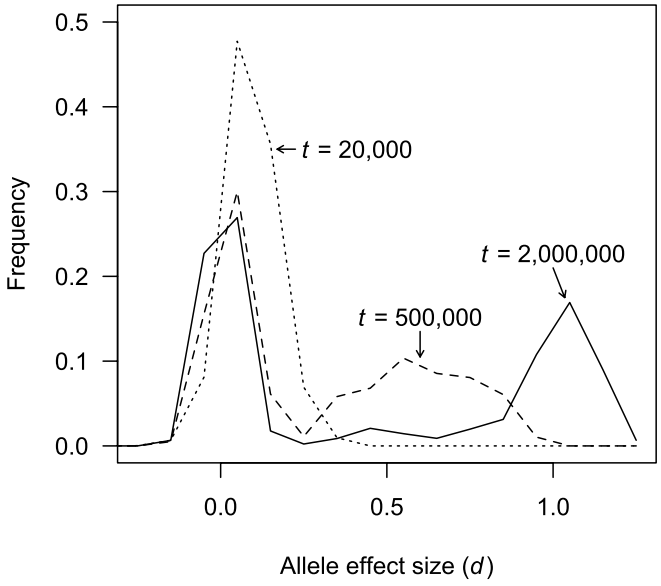

Figure 4. Frequency distributions of the sizes of alleles differentiated between the two patches (*d*) at three different time points (*t* generations). Parameters are as shown in Figure 3B, but with $\mu = 10^{-5}$ (the transition to more concentrated architectures occurs much faster with more loci or higher mutation rates). This distribution was calculated from a simulated QTL experiment via crosses of one individual from each patch. The experiment records the distribution of all homozygous differences between the parents.

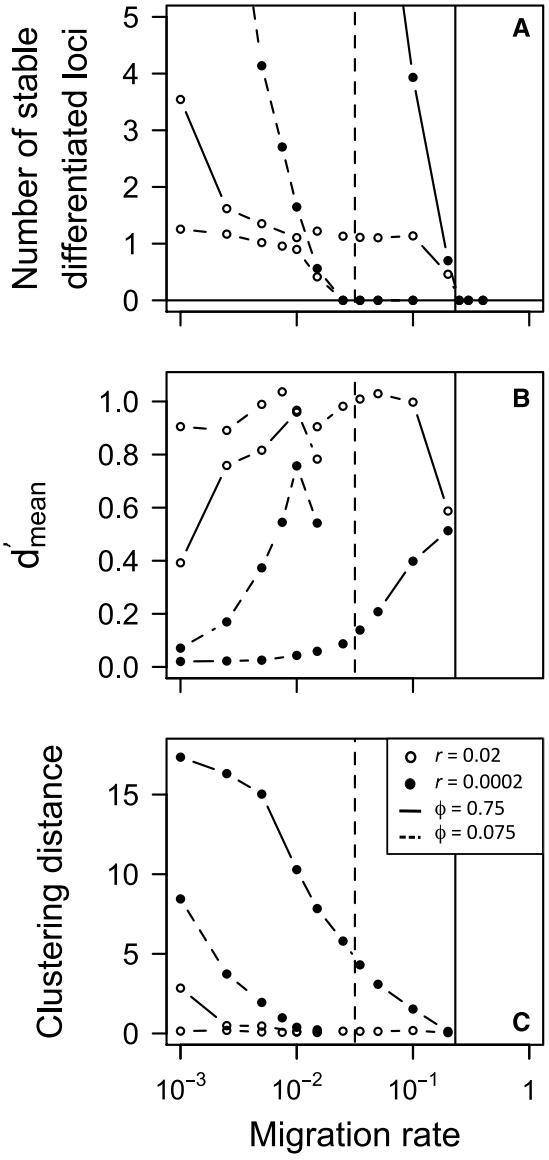

Figure 5. Effect of selection, migration, and recombination on the number of loci with stable polymorphisms contributing to divergence (A), the average size of the alleles involved (B), and the average clustering distance between them (C). When the rate of recombination is high ($r = 0.02$; circles), architectures tend to be highly concentrated, with a single pair (A) of large alleles (B) often contributing most of the divergence. When recombination is more restricted ($r = 0.0002$; dots), clusters of locally adaptive alleles contribute to adaptation, occurring over larger regions of the chromosome under stronger selection (C). In all cases, as the migration rate increases, the number of loci involved decreases (A), the average size of alleles increases (B) and the clustering distance decreases (C), indicating that more concentrated architectures are favored. Selection coefficients are $\phi = 0.75$ (solid line); $\phi = 0.075$ (dashed line). In all cases, $\mu = 10^{-4}$; $\sigma = 0.05$; $N = 1000$ and there are $n = 50$ loci. The vertical lines indicate the position of the m^Z_{crit} thresholds, evaluated for invasion versus a genotype of 0. At the lowest migration rates and $r = 0.0002$, divergence occurred at nearly all 50 loci.

recombination is relatively high ($r = 0.02$), genetic architectures tend to be characterized by divergence at either only one locus or a few loci in a tight cluster, with alleles of large effect, even though the average size of new mutations is small ($\sigma = 0.05$; 10 mutations of size $\alpha = 0.05$ are required to build locally optimal phenotypes in each patch). When recombination is lower ($r = 0.0002$), many more loci are involved in long-term divergence between populations (Fig. 5A), with clusters of locally adapted alleles extending further across the simulated region of the chromosome (Fig. 5C). When selection is strong and recombination is low ($\phi = 0.75$; $r = 0.0002$), loosely linked clusters evolve, but there is little advantage to having even more tightly linked arrangements (as shown in Fig. 2), so clusters persist across wider regions of the chromosome than under weaker selection, $\phi = 0.75$ (Fig. 5C). When migration is low ($m \sim 0.001$), these arrangements sometimes include locally deleterious alleles hitchhiking in tight linkage with the beneficial alleles, creating a locally optimal haplotype (see Supporting information, Fig. S1 for single-simulation plots similar to those in Fig. 3).

To summarize, we see increasingly concentrated architectures as $m \rightarrow m^Z_{crit}$, which is consistent with Kirkpatrick and Barton (2006) and with our predictions based on equation (4) and Figure 2. This likely occurs for two reasons: the advantage of tighter clustering between locally adapted alleles increases with

migration (up to m^Z_{crit}; as per Fig. 2) and the relative advantage of larger alleles over smaller alleles in finite populations increases as $m \to m^Z_{crit}$ (as shown in Fig. 1). We also see clustering of locally adaptive alleles maintained across much greater regions of the chromosome when selection is strong (Fig. 5C), as expected from Figure 2. This effect of the strength of selection could also be predicted from Eq. (3) of Kirkpatrick and Barton (2006), although they did not focus on this interpretation, as they were concerned with the spread of inversions that would completely eliminate recombination. Because selection partly defines the magnitude of the critical migration threshold, it also affects the range of migration rates over which there is an increased benefit to concentrated architectures. The strength of selection thus affects genetic architecture in two ways: through its primary effect defining the critical migration threshold and therefore the range in migration rate over which concentrated architectures are favored, and through a secondary effect on the physical distance on the chromosome across which there is an advantage for stable clusters of linked alleles to contribute to adaptation (as per Barton and Bengtsson 1985; Bengtsson 1985). This secondary effect is of fundamental importance to determining the extent of the chromosome that can be captured to build a "genomic island of divergence" (reviewed in Nosil et al. 2009). Generally speaking, there is a higher probability of concentrated architectures occurring in more strongly selected traits, as the larger physical regions of the chromosome that can be maintained in tight linkage are more likely to include loci that could mutate to locally beneficial alleles.

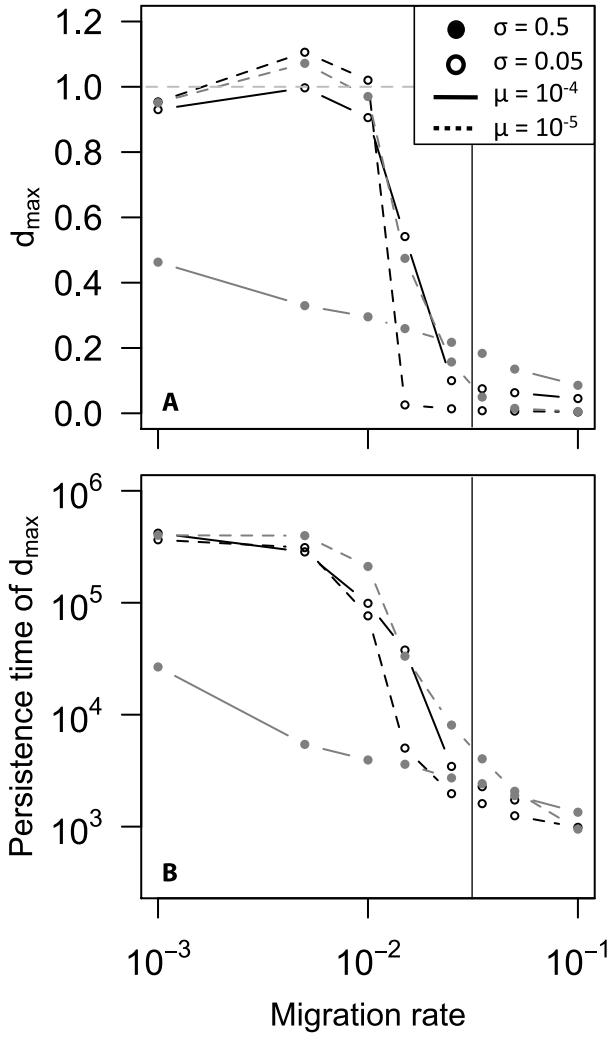

Figure 6. Influence of mutation rate and effect size on the average size of allelic divergence at the locus with the largest effect (d_{max}; A) and the maximum persistence time of d_{max} (B). Mutation rates are $\mu = 10^{-4}$ (solid lines); $\mu = 10^{-5}$ (dashed); effect sizes are $\sigma = 0.5$ (gray lines; dots); $\sigma = 0.05$ (black lines; circles), as indicated in the legend. In all cases, $r = 0.02$, $n = 50$ loci, $\phi = 0.075$, $N = 1000$. The solid vertical line indicates the position of the m^Z_{crit} threshold, evaluated for invasion versus a genotype of 0. For all cases, persistence time of d_{max} was measured during the first 500,000 generations only.

MUTATION RATE AND EFFECT SIZE

Although the effects of selection, migration, and recombination described above were predicted by our analytical theory, variations in the mutation rate and effect size result in some unexpected patterns. Somewhat surprisingly, when individual mutations are smaller on average ($\sigma = 0.05$ vs. 0.5), the architecture underlying local adaptation tends to be characterized by divergence at fewer loci with larger effect alleles that persist for longer periods of time than when individual mutations are large (Fig. 6). The large-effect alleles built by stacking when individual mutations are smaller ($\sigma = 0.05$) thus tend to have very long persistence times, whereas when individual mutations are larger and frequent ($\sigma = 0.5, \mu = 10^{-4}$), large mutations occur commonly and more rapidly replace alleles of similar effect size at other loci (Fig. 6B). Higher per-locus mutation rates have little effect when average mutation effect sizes are small ($\sigma = 0.05$), but result in cycling of the alleles contributing to divergence when effect sizes are large ($\sigma = 0.5$; Fig. 6B), along with a lower average size of $d_{\max}$ and therefore an increased number of loci involved in divergence (Fig. 6A; see Supporting information, Fig. S2 for single-simulation plots similar to those in Fig. 3). We note that when mutations are small ($\sigma = 0.05$), concentration of genetic architectures occurs more slowly when mutations rates are lower (e.g., Fig. S2).

Interestingly, in some cases the maximum size of allelic divergence (d_{max}) surpasses the optimal effect size (Fig. 6A; $d > \theta$). Unlike the architectures with many opposing alleles of large effect that occur below the drift threshold at very low m (e.g., Figs. 3 A,D), however, these architectures occur at high migration rates, just below the critical threshold, and do not have coevolved alleles that oppose the extreme effect (i.e., the sum of all values of d also exceeds the optimum; $\sum_i^n d_i > \theta$). These

alleles of extreme effect do not tend to evolve when mutations are common (Fig. 6A). We confirmed that these extreme effect alleles still occur if the phenotype is determined by a single locus (Fig. S3), but that they are sensitive to the curvature of the fitness function, and do not occur when $\gamma \leq 1$. This suggests that extreme effect alleles are a consequence of evolution at subcritical migration rates when intermediate phenotypes have higher than average fitness. We also note that the qualitative predictions about the evolution of concentrated genetic architectures under migration–selection–drift balance still hold when $\gamma < 1$ (see Fig. S4).

We also found that mutation rate had a substantial effect on the stability of concentrated architectures at larger population sizes. When population size was $N = 10^4$, concentration of architectures still occurred under strong selection ($\phi = 0.75$; Fig. 7). But when selection was weaker ($\phi = 0.075$), the rapid cycling of alleles that prevented concentration under larger mutation effect sizes and higher rates at $N = 10^3$ (Fig. 6; $\sigma = 0.5$, $\mu = 10^{-4}$), also occurred for smaller mutation effect sizes when $N = 10^4$ ($\sigma = 0.05$; Fig. 7). Reducing the rate of mutation to $\mu = 10^{-5}$ increased the persistence time of divergent mutations (Fig. 7B, dashed lines, asterisks vs. dots), restoring the concentration pattern (Fig. 7A; see Fig. S5 for single-replicate plots). When $N = 10^2$, we did not see any concentration of architectures under weaker selection (Fig. 7A), as phenotypic divergence collapses quickly after it establishes due to migration and drift and there is little stable divergence (Figs. 7B; S5B,G). Importantly, these results show that concentration of architectures is a robust pattern that occurs across a range of population sizes.

Taken together, the results in Figures 6 and 7 show that the availability of mutations of large effect has considerable influence on the shape and temporal stability of the genetic architecture of local adaptation. Although small effect mutations may be unable to contribute to local adaptation when $m^{\alpha}_{crit} < m < m^{Z}_{crit}$, if the genome is flexible enough to permit clustering or stacking, then this constraint can be overcome by the creation of large effect alleles by multiple mutations at a single gene or by mutations at multiple loci in tight linkage.

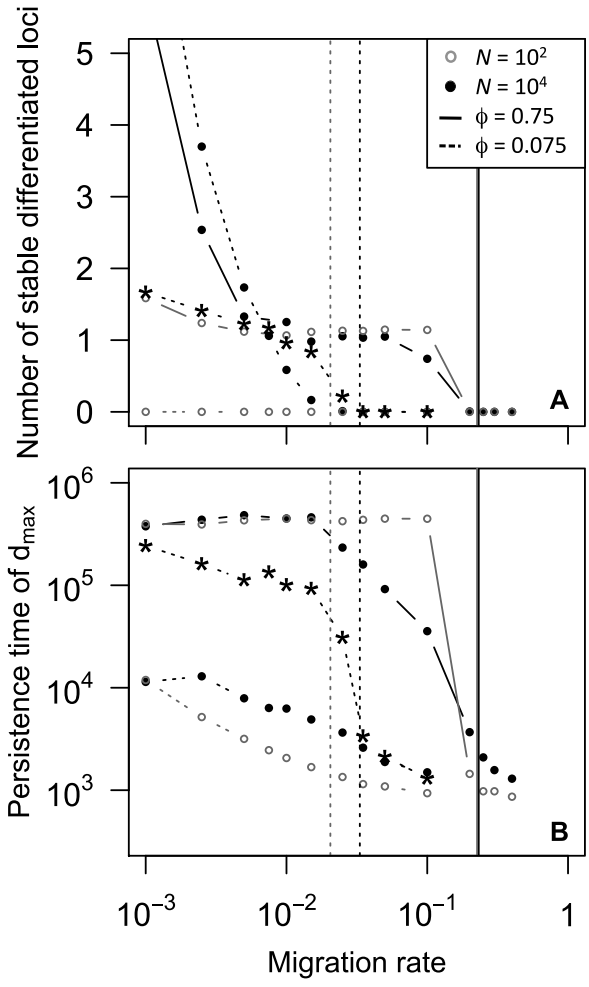

Figure 7. Influence of population size (*N*) on number of differentiated loci contributing to divergence between populations. Mutation rate per locus is $\mu = 10^{-4}$ in all cases except asterisks, where $\mu = 10^{-5}$ and $N = 10^4$. Recombination rate is $r = 0.02$; all other parameters are as in Figure 5 or as shown in the legend.

Discussion

Migration–selection balance in finite populations tends to result in genetic architectures that minimize the number of loci or linkage groups involved in local adaptation. In light of these findings, we would expect traits under migration–selection–drift balance to have fewer QTL with higher percent variance explained (PVE) by each locus than traits under purifying or directional selection without migration, all else being equal. As such, although the relatively common finding of large effect QTL underlying locally adaptive traits may simply be a product of their increased probability of discovery, it might also be a direct consequence of their relative advantage under migration–selection balance in finite populations. These results thus have implications for predicting the number of undetected small effect QTL underlying a locally adaptive trait (e.g., Otto and Jones 2000; Hayes and Goddard 2001). The distributions of allele effect size observed in this study have many fewer alleles of small and intermediate effect (Fig. 4) than expected from an exponential distribution (e.g., Orr 1998), suggesting caution in making assumptions about the expected distribution of QTL effect sizes for traits evolving under migration–selection balance. Interestingly, we also found much more concentrated architectures than reported by Griswold (2006), who used a similar individual-based model. Where Griswold suggested that "it is unexpected to find alleles of large effect when populations have diverged for a long period of time

and their phenotypic optima are far apart" (2006; p. 452), we find that given sufficient time, concentrated architectures with most of the divergence contributed by a single locus will evolve even when mutations are very small relative to the difference in optimum (Fig. 6). Our study examined changes in architecture over much longer periods of time than that of Griswold (>500,000 vs. 10,000 generations), during which we observed a steady increase in d_{max} and a concomitant decrease in the number of loci involved in adaptive divergence (Fig. 3B,E), which would seem to account for the more concentrated architectures observed in our study. Also, Griswold did not allow recurrent mutations at a single locus and did not examine whether locally adapted alleles were tending to cluster in tight linkage groups, which might also explain some of the difference in our results.

We note that van Doorn and Dieckman (2005), Kopp and Hermisson (2006), and Schneider (2007) also found concentrated architectures evolving under frequency-dependent disruptive selection without migration, but that in some cases this depended on the mutation model and assumptions. Kopp and Hermisson (2009) also found marked deviations from the exponential distributions expected by Orr (1998) when populations evolved toward a moving rather than static optimum. By contrast, Martin et al. (2006) showed that increased recombination can be favored when populations evolve toward a new optimum (without migration), implying that less-concentrated architectures might be favored in the absence of spatially heterogeneous selection. As such, it would be interesting to compare the architecture of adaptation under other selection regimes (e.g., alternating temporal and/or spatial variation in optimum), and to incorporate epistasis, which can also favor less-concentrated architectures (Lenormand and Otto 2000), to explore the robustness of these patterns. Similarly, as we rely upon the restrictive assumptions of symmetrical migration rates and strengths of selection, it would be interesting to explore the effect of more biologically realistic population structures on the generality of these results.

The expectation of selection for reduced recombination between locally adapted loci has been previously been discussed by Lenormand and Otto (2000) as a mechanism affecting genetic architecture. The expectation of tightly linked selected loci is also implicit in other studies on the evolution of recombination, which have concluded that recombination is disfavored under divergent selection and migration when there is no epistasis within patches, as this minimizes the load created when locally adapted genotypes recombine with maladapted immigrant genotypes (Maynard Smith 1977; Pylkov et al. 1998; Lenormand and Otto 2000). These papers predict under these circumstances that stronger selection for reduced recombination will occur as the migration rate is increased from zero and under stronger selection for the locally adapted loci. These are the same conditions under which we observe the evolution of more tightly clustered locally adapted alleles.

Clustering of reproductive isolating mechanisms into "islands of genomic divergence" is also predicted in models of chromosomal speciation (Noor et al. 2001; Rieseberg 2001; Navarro and Barton 2003; Gavrilets 2004; Nosil et al. 2009). Kirkpatrick and Barton (2006) showed that the net strength of selection favoring the elimination of recombination between previously unlinked loci (e.g., by an inversion) is proportional to the migration rate and number of loci involved in local adaptation. Our analytical and simulation results are consistent with this predicted effect of migration, and also show a biologically interesting interaction between selection and recombination (see Results). In their recent comparison of differentiation between locally adapting populations at inverted versus uninverted genomic regions, Feder and Nosil (2009) showed that there was little difference in the equilibrium frequency achieved by these alternate rearrangements (gray vs. black lines in their Fig. 2, which would correspond to $r = 0.5$ and $r = 0$ in our model). Although focusing on differences in equilibrium frequency suggests a small effect of genetic architecture, our results show that if different architectures are competing, concentrated architectures will tend to replace more diffuse ones, indicating a substantial effect of linkage during local adaptation.

Our results can also be interpreted in light of Haldane's (1957) work on the cost of selection, which showed that the number of selective deaths (and therefore the migration load) associated with maintaining differences between populations should be proportional to the number of locally maladapted alleles entering a population per generation. If fewer loci are responsible for divergence, then the migration load imposed on the populations will also be proportionately less as a result.

The evolution of concentrated architectures can occur through processes operating at two potentially overlapping timescales: (1) At the outset of a bout of local adaptation (or following the homogenization of a previously existing divergence), the establishment of a single locally adapted allele can facilitate the recruitment of other locally adapted alleles in tight linkage, potentially allowing the establishment of small effect alleles that would not otherwise contribute to divergence when $m > m^{\alpha}_{crit}$ (similar to the growth of "genomic islands of divergence"; Nosil et al. 2009). These new alleles potentially increase the effectiveness of divergent selection in this region, making it even easier for subsequent linked alleles to invade locally. This process is strongest when mutations of large effect are rare, because otherwise divergence can occur without need for support from other diverged loci. (2) Once locally adaptive alleles have arisen, a diffuse architecture might be replaced by a more concentrated architecture arising either through the invasion of a new mutation in tight linkage to an existing allele (with subsequent homogenization of

previously established divergent alleles at more loosely linked loci) or through some sort of genomic rearrangement increasing the linkage between locally adapted alleles (e.g., translocation, chromosome inversion, or transposon mediated gene movement). Although the sequence of genetic events involved in these paths to more concentrated architectures differ, in both cases concentrated architectures evolve because they increase the stability of combinations of locally adapted alleles. There are two reasons that concentrated architectures are favored, depending on the circumstances: an advantage of tight linkage that is independent of population size (Fig. 2), and an advantage of larger/more tightly linked arrangements in finite populations (Fig. 1). Although we do not distinguish between the relative importance of these in the simulation results, we find that concentrated architectures will evolve at both relatively small and large population sizes (Fig. 7). Whatever the mechanism by which concentrated architectures eventually arise, our study suggests that they are a robust consequence of evolution under prolonged periods of migration–selection balance in finite populations.

VIOLATION OF THE GAUSSIAN ASSUMPTION OF QUANTITATIVE GENETICS

The general finding that concentrated architectures are favored under migration–selection–drift balance has important implications for modeling the evolution of quantitative traits. Yeaman and Guillaume (2009) showed that although simulations using an equal-effect diallelic model with free recombination would agree well with the predictions of a quantitative genetic model (Hendry et al. 2001), considerable genetic skew could be generated under either decreased recombination among alleles or heterogeneity in allele effect sizes, causing the quantitative genetic model to underestimate divergence under migration load. Here, we show that these very architectures that facilitate the generation of skew are those that are most likely to evolve under migration—selection–drift balance (i.e., tight linkage and/or few large effect alleles). It would therefore seem that quantitative genetic models assuming a Gaussian distribution of genotypes may be inherently unsuitable for modeling migration–selection processes, as this process results in architectures that facilitate the generation of skew, thereby violating the common quantitative genetic assumption of Gaussian-distributed breeding values. The effect of deviations from normality under strong selection has been discussed extensively by Turelli and Barton (1990, 1994).

UNEXPECTED PATTERNS CAUSED BY STOCHASTIC DYNAMICS

Exploring the evolution of genetic architecture in finite populations using individual-based simulations also reveals some unpredicted patterns. First, there is often an inverse relationship between the size of individual mutations and the size of the stable alleles/linkage groups that contribute to long-term divergence (Fig. 6). When mutations have small effects, their individual persistence time is low and they tend to be lost due to migration and drift more frequently (Yeaman and Otto 2011). We have shown here that clustering into tighter linkage groups or stacking of mutations can greatly increase persistence time, especially if average-sized mutations are not sufficiently large to surpass the critical threshold, as shown in Figure 1. When individual mutations are small and rare, it is rare for another large allele or cluster to evolve and displace the resident cluster (as this requires multiple mutational steps in rapid succession); as such, architectures are stable over long periods of time (Fig. 6B). Alternatively, when mutations are large and occur frequently, they tend to cycle through the population because it is easy for an allele of similar size to arise by a single mutation and drift to high frequency (as alleles of the same size are neutral with respect to each other). As a result, at high mutation rates and large effect sizes, individual alleles rarely persist for long enough for clusters to be of much importance (Fig. 6). This has implications for the extension of our results to more complicated metapopulation structure, as the rate and size of mutations might greatly affect the variation among patches in evolved genetic architecture. In his recent examination of a multipatch deterministic migration–selection model, Bürger (2009, 2010) has shown that as many alleles can be maintained at each locus as there are patches in a metapopulation, although the likelihood of this sort of variation in architecture in finite populations is unclear and may depend heavily on the dynamics discussed above.

Another unpredicted pattern observed in the simulations was the evolution of alleles and chromosomes with extreme effects when m was just below the m^Z_{crit} threshold and when $\gamma > 1$, resulting in genotypes that surpassed the local optimum in the homozygous state (Supporting information), especially when mutation rates were low (Fig. 6). The explanation for this is as follows: when locally optimal alleles are segregating in each patch (i.e., $\alpha = \pm 0.5$) at subcritical migration rates, the maladaptive immigrant alleles/genotypes reach relatively high frequencies, resulting in high frequencies of hybrid individuals. When there is a high frequency of hybrid individuals, an extreme effect allele (i.e., $\alpha > |0.5|$) can invade where it is locally favored, because the fitness advantage in its heterozygous state can exceed the fitness disadvantage in its homozygous state when the fitness function has a convex curvature ($\gamma = 2$). For example, under a selection regime of $\phi = 0.75$, $\theta = 1$, and $\gamma = 2$, when the resident allele $\alpha_r = 0.5$ and the invading extreme allele, $\alpha_e = 0.6$, the relative fitness of α_e versus α_r would be 1.044 in the heterozygous state versus 0.9925 in the homozygous state. As long as migration is high enough to maintain a large number of heterozygotes, α_e would invade and replace α_r. This would result in strong selection for an opposing extreme allele with $\alpha_e = -0.6$ to invade in the other

patch. Once both extreme alleles are established, the heterozygous benefit would be nullified, as the phenotype produced by two opposing extreme alleles would again be zero. Although an optimal nonextreme allele could then reinvade, this would again generate the advantage for re-invasion by another extreme allele. Extreme genotypes are thus a robust phenomenon under finite population sizes and convex fitness functions, especially when mutation rates are low, as shown in Figure 6. It would be interesting to see whether these extreme genotypes are ever observed in nature.

CONCLUSIONS AND FUTURE DIRECTIONS

Taken together, these results suggest that migration–selection–drift balance in finite populations should typically result in the evolution of concentrated genetic architectures with distributions of differentiated allele effect size that are dramatically different from the predictions of Orr (1998) and Griswold (2006). The most significant constraint to the evolution of such concentrated architectures may be a limitation in the number of possible beneficial mutations occurring in tight enough linkage to build a locally adapted phenotype. Clusters of locally adapted alleles can be maintained over greater physical distances on the chromosome under reduced recombination or stronger selection, so if there are only a limited number of ways for mutations to build a phenotype, stable concentrated architectures are more likely under these conditions. Although we formulated a model with a single trait under selection, multiple traits would likely exhibit similar patterns, with alleles adapting to the same environmental conditions tending to cluster together regardless of the specific trait they affect. Moreover, with pleiotropy, alleles of small effect on a focal trait can differentiate as a result of stronger selection on their effect on other traits.

If migration–selection–drift balance actually plays a strong role in the evolution of genetic architecture, we can predict some broad patterns at the genomic level. If successive bouts of local adaptation under migration load have favored the spread of genomic rearrangements to create clusters of more tightly linked locally adaptable genes, then genes for traits often involved in local adaptation (e.g., phenology, water-use efficiency, or temperature tolerance) may tend cluster more closely around each other than observed for a random sample of genes. Lineages with these sorts of rearrangements would be better able to adapt to the challenges posed by heterogeneous environments, potentially increasing their long-term survival or their propensity to speciate. However, we have not explicitly modeled such species selection.

There are still little empirical data upon which we can test these hypotheses, although a recent review of clustering of F_{ST} outlier loci assumed to experience divergent selection, Nosil et al. (2009) documented a range of patterns (from weakly to strongly clustered) in five studies that had mapped these loci. A more direct way to test for the importance of migration on the evolution of genetic architecture would be to compare the genetic basis of local adaptation within and among isolated island populations versus interconnected mainland populations or closely related selfing versus outcrossing taxa (as the rate of recombination should be much lower in selfing taxa). Another promising avenue of study would be to compare the potential number of loci that could contribute to adaptation (as indicated by an artificial selection experiment) to the actual number of QTL observed in divergent populations adapting to similar stresses in the wild. As this field of research is still in its infancy, further empirical work is required to explore whether migration commonly affects the genetic architecture of local adaptation.

ACKNOWLEDGMENTS

This work developed in close relation to other projects with S. Otto and F. Guillaume, who provided helpful comments and discussion throughout. We would also like to thank N. Barton, D. Schluter, L. Rieseberg, D. Irwin, R. Bürger, A. Schick, A. Blachford, B. Davis, T. Lenormand, J. Willis, and anonymous reviewers for their contributions and suggestions. This work was supported by an NSERC Discovery Grant to MCW, an NSERC PGS-D to SY, and a grant to L. Lehmann (PP00P3-123344; Swiss NSF).

LITERATURE CITED

Albert, A. Y. K., S. Sawaya, T. H. Vines, A. K. Knecht, C. T. Miller, B. R. Summers, S. Balabhadra, D. M. Kingsley, and D. Schluter. 2006. The genetics of adaptive shape shift in stickleback: pleiotropy and effect size. Evolution 62:76–85.

Barton, N., and B. O. Bengtsson. 1986. The barrier to genetic exchange between hybridizing populations. Heredity 56:357–376.

Bengtsson, B. O. 1985. The flow of genes through a genetic barrier. Pp. 31–42 *in* J. J. Greenwood, P. H. Harvey, and M. Slatkin, eds. Evolution essays in honour of John Maynard Smith. Cambridge Univ. Press, Cambridge.

Bradshaw Jr., H. D., S. M. Wilbert, K. G. Otto, and D. W. Schemske. 1995. Genetic mapping of floral traits associated with reproductive isolation in monkeyflowers (*Mimulus*). Nature 376:762–765.

Bradshaw, Jr. H. D., K. G. Otto, B. E. Frewen, J. K. Mckay, and D. W. Schemske. 1998. Quantitative trait loci affecting differences in floral morphology between two species of monkeyflower (*Mimulus*). Genetics 149:367–382.

Bulmer, M. G. 1972. Multiple niche polymorphism. Am. Nat. 106:254–257.

Bürger, R. 2009. Multilocus selection in subdivided populations II. Maintenance of polymorphism under weak or strong migration. J. Math. Biol. 58:979–997.

———. 2010. Polymorphism in the two-locus Levene model with nonepistatic directional selection. Theor. Popul. Biol. 76:214–228.

Buckler, E. S., J. B. Holland, P. J. Bradbury, C. B. Acharya, P. J. Brown, C. Browne, E. Ersoz, S. Flint-Garcia, A. Garcia, J. C. Glaubitz, et al. 2009. The genetic architecture of maize flowering time. Science 325:714–718.

Christians, J. K., and L. K. Senger. 2007. Fine mapping dissects pleiotropic growth quantitative trait locus into linked loci. Mammal. Genome 18:240–245.

Colosimo, P. F., C. L. Peichel, K. Nereng, B. K. Blackman, M. D. Shapiro, D. Schluter, and D. M. Kingsley. 2004. The genetic architecture of parallel

armor plate reduction in threespine sticklebacks. PLOS Biol. 2:0635–0641.

Feder, J. L., and P. Nosil. 2009. Chromosomal inversions and species differences: when are genes affecting adaptive divergence and reproductive isolation expected to reside within inversions? Evolution 63:3061–3075.

Gavrilets, S. 2004. Fitness landscapes and the origin of species. Princeton Univ. Press, Princeton, NJ.

Griswold, C. K. 2006. Gene flow's effect on the genetic architecture of a local adaptation and its consequences for QTL analyses. Heredity 96:445–453.

Guillaume, F., and J. Rougemont. 2006. Nemo: an evolutionary and population genetics programming framework. Bioinformatics 22:2556–2557.

Haldane, J. B. S. 1930. A mathematical theory of natural and artificial selection. Part VI. Isolation. Proc. Cambridge Philos. Soc. 26:220–230.

Haldane, J. B. S. 1957. The cost of natural selection. J. Genet. 55:511–524.

Hayes, B., and M. E. Goddard. 2001. The distribution of the effects of genes affecting quantitative traits in livestock. Genetic Selection Evol. 33:209–229.

Hedrick, P. W., M. E. Ginevan, and E. P. Ewing. 1976. Genetic polymorphism in heterogeneous environments. Annu. Rev. Ecol. Syst. 7:1–32.

Hendry, A. P., T. Day, and E. B. Taylor. 2001. Population mixing and the adaptive divergence of quantitative traits in discrete populations: A theoretical framework for empirical tests. Evolution 55:459–466.

Howe, G. T., S. N. Aitken, D. B. Neale, K. D. Jermstad, N. C. Wheeler, and T. H. H. Chen. 2003. From genotype to phenotype: unraveling the complexities of cold adaptation in forest trees. Can. J. Bot. 81:1247–1266.

Kirkpatrick, M., and N. Barton. 2006. Chromosome inversions, local adaptation, and speciation. Genetics 173:419–434.

Kopp, M., and J. Hermisson. 2006. The evolution of genetic architecture under frequency-dependent disruptive selection. Evolution 60:1537–1550.

———. 2009. The genetic basis of phenotypic adaptation II: the distribution of adaptive substitutions in the moving optimum model. Genetics 183:1453–1476.

Lenormand, T., and S. P. Otto. 2000. The evolution of recombination in a heterogeneous environment. Genetics 156:423–438.

Lenormand, T. 2002. Gene flow and the limits to natural selection. Trends Ecol. Evol. 17:183–189.

Linhart, Y. B., and M. C. Grant. 1996. Evolutionary significance of local genetic differentiation in plants. Annu. Rev. Ecol. Syst. 27:237–277.

Lythgoe, K. A. 1997. Consequences of gene flow in spatially structured populations. Genet. Res. Cambridge 69:49–60.

Lopez, S., F. Rousset, F. H. Shaw, R. G. Shaw, and O. Ronce. 2008. Migration load in plants: role of pollen and seed dispersal in heterogeneous landscapes. J. Evol. Biol. 21:294–309.

McGregor, A. P., V. Orgogozo, I. Delon, J. Zanet, D. G. Srinivasan, F. Payre, and D. L. Stern. 2007. Morphological evolution through multiple *cis*-regulatory mutations at a single gene. Nature 448:587–591.

Martin, G., S. P. Otto, T. Lenormand. 2006. Selection for recombination in structured populations. Genetics 172:593–609.

Maynard Smith, J. 1977. Why the genome does not congeal. Nature 268:693–696.

Navarro, A., and N. H. Barton. 2003. Accumulating postygotic isolation genes in parapatry: a new twist on chromosomal speciation. Evolution 57:447–459.

Noor, M. A. F., K. L. Grams, L. A. Bertucci, and J. Reiland. 2001. Chromosomal inversions and the reproductive isolation of species. Proc. Natl. Acad. Sci. USA 98:12084–12088.

Nosil, P., D. J. Funk, and D. Ortiz-Barrientos. 2009. Divergent selection and heterogeneous genomic divergence. Mol. Ecol. 18:375–402.

Orr, H. A. 1998. The population genetics of adaptation: the distribution of factors fixed during adaptive evolution. Evolution 52:935–949.

———. 2001. The genetics of species differences. Trends Ecol. Evol. 16:343–350.

Otto, S. P., and C. D. Jones. 2000. Detecting the undetected: estimating the total number of loci underlying a quantitative trait. Genetics 156:2093–2107.

Pylkov, K. V., L. A. Zhivotovsky, and M. W. Feldman. 1998. Migration versus mutation in the evolution of recombination under multilocus selection. Genet. Res. Cambridge 71:247–256.

Rieseberg, L. 2001. Chromosomal rearrangements and speciation. Trends Ecol. Evol. 16:351–358.

Schneider, K. A. 2007. Long-term evolution of polygenic traits under frequency-dependent intraspecific competition. Theor. Popul. Biol. 71:342–366.

Shapiro, M. D., M. E. Marks, C. L. Peichel, B. K. Blackman, K. S. Nereng, B. Jońsson, D. Schluter, and D. M. Kingsley. 2004. Genetic and developmental basis of evolutionary pelvic reduction in threespine sticklebacks. Nature 428:717–723.

Slate, J. 2005. Quantitative trait locus mapping in natural populations: progress, caveats, and future directions. Mol. Ecol. 14:363–379.

Spichtig, M., and T. J. Kawecki. 2004. The maintenance (or not) of polygenic variation by soft selection in heterogeneous environments. Am. Nat. 164:70–84.

Steiner, C., J. N. Weber, and H. E. Hoekstra. 2007. Adaptive variation in beach mice produced by two interacting pigmentation genes. PLOS Biol. 5:1880–1889.

Turelli, M., and N. H. Barton. 1990. Dynamics of polygenic characters under selection. Theor. Popul. Biol. 38:1–57.

———. 1994. Genetic and statistical analyses of strong selection on polygenic traits: what, me normal? Genetics 138:913–941.

van Doorn, G. S., and U. Dieckman. 2005. The long-term evolution of multilocus traits under frequency-dependent disruptive selection. Evolution 60:2226–2238.

Wright, S. 1931. Evolution in Mendelian populations. Genetics 16:97–159.

Yeaman, S., and F. Guillaume. 2009. Predicting adaptation under migration load: the role of genetic skew. Evolution 63:2926–2938.

Yeaman, S., and S. P. Otto. 2011. Establishment and maintenance of adaptive genetic divergence under migration, selection, and drift. Evolution. doi:10.1111/j.1558-5646.2011.01277.x [Epub ahead of print].

Associate Editor: N. Barton

Supporting Information

The following supporting information is available for this article:

Figure S1. Evolution of genetic architecture over the first 500,000 generations of a single simulation replicate for the four-parameter combinations from Figure 5 of the article.

Figure S2. Evolution of genetic architecture over the first 500,000 generations of a single simulation replicate for the four-parameter combinations from Figure 6 of the article.

Figure S3. Average difference in effect size between the leading alleles in each population for a quantitative trait determined by a single locus ($\bar{d}$), for three different curvatures of the fitness function (γ).

Figure S4. Effect of the curvature of the fitness function on the number of loci with stable polymorphisms contributing to divergence (A), the average size of the alleles involved (B), and the average clustering distance between them (C).

Figure S5. Evolution of genetic architecture over the first 500,000 generations of a single simulation replicate for the parameter combinations from Figure 7 of the article (with $m = 10^{-3}$).

Supporting Information may be found in the online version of this article.